Accepted Manuscript

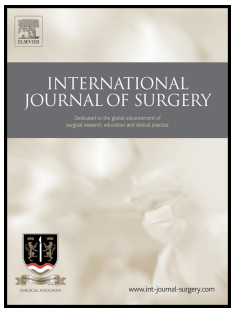

Pancreatic tumors: Imaging update 2015

Michele Scialpi, MD, Alfonso Reginelli, MD, Sabrina Gravante, MD, Giuseppe Falcone, MD, Paolo Baccari, MD, Lucia Manganaro, MD, Barbara Palumbo, MD, Salvatore Cappabianca, MD

PII: S1743-9191(15)01439-9

DOI: 10.1016/j.ijsu.2015.12.053

Reference: IJSU 2426

To appear in: *International Journal of Surgery*

Please cite this article as: Scialpi M, Reginelli A, Gravante S, Falcone G, Baccari P, Manganaro L, Palumbo B, Cappabianca S, Pancreatic tumors: Imaging update 2015, *International Journal of Surgery* (2016), doi: 10.1016/j.ijsu.2015.12.053.

Pancreatic tumors: imaging update 2015

[1]Michele Scialpi, MD, [2]Alfonso Reginelli, MD, [1]Sabrina Gravante, MD, [1]Giuseppe Falcone, MD, [3]Paolo Baccari , MD, [4]Lucia Manganaro, MD, [5]Barbara Palumbo, MD, [2]Salvatore Cappabianca, MD

[1]Department of Surgical and Biomedical Sciences, Division of Radiology 2, Perugia University, S. Maria della Misericordia Hospital, S. Andrea delle Fratte, 06134, Perugia, Italy.

[2]Department of Internal and Experimental Medicine, Magrassi-Lanzara, Institute of Radiology, Second University of Naples, Naples, Italy Piazza Miraglia 2 80138 Napoli

[3]Department of Radiology, Sapienza University of Rome, Viale Regina Elena 324 00161, Rome, Italy

[4]Department of Surgical and Biomedical Sciences, Division of Radiology 2, Perugia University, S. Maria della Misericordia Hospital, S. Andrea delle Fratte, 06134, Perugia, Italy.

[5]Division of Surgery, S. Maria della Misericordia Hospital, S. Andrea delle Fratte, 06134, Perugia, Italy

Corresponding Author: Salvatore Cappabainca, MD

Department of Internal and Experimental Medicine, Magrassi-Lanzara,

Institute of Radiology, Second University of Naples, Naples, Italy

Piazza Miraglia 2 80138 Napoli

E-mail: salvatore.cappabianca@unina2.it

ABSTRACT

Today, ultrasound (US), computed tomography (CT) and Magnetic Resonance imaging (MRI) repesent the mainstay in the evaluation of pancreatic solid and cystic tumors affecting pancreas in 80-85% and 10-15% of the cases respectively . Integration of US, CT or MR imaging is essential for an accurate assessment of pancreatic parenchyma, ducts and adjacent soft tissues in order to detect and to stage the tumor, to differentiate solid from cystic lesions and to establish an appropriate treatment. The purpose of this review is to provide an overview of pancreatic tumors and the role of imaging in their diagnosis and management.

In order to a prompt and accurate diagnosis and appropriate management of pancreatic lesions, it is crucial for radiologists to know the key findings of the most frequent tumors of the pancreas and the current role of imaging modalities.

A multimodality approach is often helpful. If MDCT is the preferred initial imaging modality in patients with clinical suspicion for pancreatic cancer, multiparametric MRI provides essential information for the detection and characterization of a wide variety of pancreatic lesions and can be used as a problem-solving tool at diagnosis and during follow-up.

Keywords: pancreas, pancreatic tumors, ultrasound (US), contrast-enhanced ultrasound (CEUS), multidetector-row computed tomography (MDCT), Split-bolus MDCT, magnetic resonance imaging (MRI), multiparametric MRI, positron emission tomography (PET).

Introduction

Today, ultrasound (US), computed tomography (CT) and Magnetic Resonance imaging (MRI) repesent the mainstay in the evaluation of pancreatic solid and cystic tumors affecting pancreas in 80-85% and 10-15% of the cases respectively [1,2]. Integration of US, CT or MR imaging is essential for an accurate assessment of pancreatic parenchyma, ducts and adjacent soft tissues in order to detect and to stage the tumor, to differentiate solid from cystic lesions and to establish an appropriate treatment. The purpose of this review is to provide an overview of pancreatic tumors and the role of imaging in their diagnosis and management.

Classification

Pancreatic tumors including a heterogeneous group of primary lesions: adenocarcinoma, neuroendocrine tumor (NET), pancreatic cystic neoplasms, solid pseudopapillary tumor, pancreatoblastoma, pancreatic lymphoma and rare miscellaneous neoplasms [1] (Table 1).

Pancreatic ductal adenocarcinoma (PDA) represent 85%-95% of all pancreatic solid pancreatic malignant neoplasms while neuroendocrine tumors are frequently benign and include insulinoma, gastrinoma, glucagonoma, somatostatinoma, vasoactive intestinal polypeptide tumor (VIPoma), Pancreatic polypeptide secreting tumors (PPomas) and non-functioning tumors, amounting to 3%-4% of the cases [1].

Clinical presentation

Early pancreatic cancer is often asymptomatic. Tumors in the pancreatic head (75% of the cases) often present early with biliary obstruction. However, tumors in the body and tail can remain asymptomatic till late in disease stage [3].

Weight loss, poor appetite, abdominal discomfort, abdominal or midback pain and obstructive jaundice and related symptoms are relatively common and generally occur late in the clinical

development; pancreatitis is less common as presenting symptoms [1,4,5]. Digestive problems, nausea and vomiting occur more frequently when the cancer presses on the stomach. Rarely, pancreatic cancers cause diabetes due to the destruction of insulin-making cells. Encasement of vascular structures, infiltration of adjacent bowel and superior mesenteric vein thrombosis may all occur later.

PDA is associated with several rare paraneoplastic syndromes: Trousseau syndrome is traditionally defined as migratory thrombo-phlebitis [6-7]. Panniculitis is associated with acinar cell carcinoma in 8% of cases; eczematous dermatitis, fibrous cutaneous hand changes, plantar keratoderma, polymyositis, neurological and hematologic manifestation represent other paraneoplastic syndromes [1,8-10].

Signs and symptoms of pancreatic functioning NET are different and dependent on an excessive secretion of hormones. Insulinoma (50%) reveals itself with hypoglycemic attacks featuring neuroglycopenia and sympathetic over-stimulation, including weakness, confusion, sweating, and rapid heartbeat, and/or atypical seizures [1,11-13]. Gastrinomas (20%) produce too much gastrin, causing a condition known as Zollinger-Ellison syndrome, resulting in peptic ulcers which can cause pain, nausea, loss of appetite and anemia [1,11,14-17]. VIPomas (3%) make vasoactive intestinal peptide (VIP) and result in watery diarrhea and hypokalemia [1,11,12,18]. Glucagonomas (1%) produces glucagon that increases glucose levels in the blood; most of the symptoms are often nonspecific, as diarrhea, weight loss, malnutrition and rarely hyperglycemia. The most distinctive feature of a glucagonoma is necrolytic migratory erythema, a red rash with swelling and blisters that often travels place to place on the skin [1,11,12, 19]. Somatostatinomas (<1%) produce somatostatin; symptoms can include diarrhea, steatorrhea, nausea, poor appetite and weight loss, gallstones, and symptoms of diabetes [1,11,20]. Ppomas cause an increase in the production of pancreatic polypeptide (PP), but they are rare and have not been associated with any clinical syndrome [21]; some patients also get watery diarrhea.

Signs and symptoms of non-functioning neuroendocrine tumors are caused by mass effect (mainly jaundice, belly pain and weight loss) [11].

Moreover, asymptomatic cancer can be incidentally detected on abdominal scans obtained for other reasons.

Imaging

Plain radiograph

Plain abdominal radiograph has a very limited role in imaging of the pancreas; sometimes it can show coarse parenchymal calcification of the pancreas in 25-59% of patients with chronic pancreatitis ; however, calcifications near the pancreas can be confused with splenic artery calcifications.

Ultrasound

Ultrasound (US) is usually limited in the evaluation of pancreas due to body habitus (adipose tissue) and the interposed intestinal and gastric bloating [22-23]. However, US is the first non-invasive imaging test for the evaluation of pancreas. Transabdominal conventional US allows to assess size, site and echogenicity of pancreatic lesions with a sensitivity and a specificity respectively of 75% [24] and an accuracy of 50%-70% [25] and to evaluate the Wirsung duct caliber. Most focal pancreatic lesions are hypoechoic compared to normal parenchyma. Typically dilatation of the common bile duct and pancreatic duct (double duct sign), which is very suggestive for a mass in the pancreatic head, even in the absence of a visible mass, is seen in patients with a pancreatic head tumor.

Endoscopic US (EUS) provides ultra-high resolution images and is commonly accepted as the most sensitive technique for detection of small pancreatic head tumors (< 2 cm) [26].

Contrast-enhanced US

The introduction of microbubble contrast agents has improved the diagnostic accuracy of US in the study of pancreatic pathologies [27,28]. Contrast-enhanced US (CEUS) is a cost-effective real-time method that allows the evaluation of the enhancement of pancreatic lesions during the dynamic phases [28] and provides useful findings for differentiating pancreatic carcinoma from chronic focal pancreatitis [29]; moreover CEUS is very accurate in demonstrating NET vascularisation [30].

Even if the Authors themselves suggest that CEUS is an accurate method for the characterization of pancreatic masses [31], CEUS is not sufficient to characterize the tumor, but rather it can improve the accuracy of US of pancreatic lesions incidentally detected as complementary dynamic imaging [30]; contrast-enhanced CT and/or MRI allow a more accurate evaluation of the local extension and metastatic spread [32,33]. Nevertheless, CEUS can be used during follow-up in patients with severe acute pancreatitis, after an initial CT evaluation, because it may help identify and delineate necrotic areas, which do not enhance [27,34].

Technique – After contrast agent injection, enhancement of the pancreas begins immediately after aortic enhancement during an early arterial phase (10 to 30 sec); subsequently there is a transient venous phase (30 to approximately 120 sec) [27]. The main limitation is represented by the different pharmacokinetics of microbubble contrast agents in comparison to the contrast medium of CT or MRI, due to their confine in vessel lumen without extravascular phase; consequently the late phase of CEUS does not correspond to the interstitial or parenchymal equilibrium phase described in CT and/or MRI [23].

Multidetector-row CT

Multidetector-row Computed Tomography (MDCT) is the most widely used imaging modality for pancreatic tumors evaluation with a sensitivity between 76%-92% for diagnosing pancreatic cancer [3,35,36]. Brennan et al. assert that CT has an accuracy of 85%–95% for tumor detection, a positive predictive value of 89%–100% for unresectability and a negative predictive value of 45%–79% for resectability [37].

MDCT allows to accurately assess tumor morphology, ductal anatomy, and its relationship to surrounding organs and vascular structures, permitting a surgical planning. High-resolution MDCT and image-processing techniques (multiplanar reconstructions and curved reformations) can provide additional details and can define the pancreatic ductal course and anatomy. CT is also easily able to detect the “double duct sign”, whereas tumors in the pancreatic body may cause upstream MPD dilatation.

Since the tumor may be isoattenuating, no pancreatic mass is visualized in 10% of cases [37].

Indirect signs, such as abrupt cut off of the pancreatic duct PD dilation (interrupted duct sign), mass effect on the pancreatic parenchyma and atrophic distal parenchyma, should be considered as indicators of tumors when mass cannot be clearly identified on CT [38]; the knowledge of pancreatic cancer and surrounding parenchyma at CT is essential to improve research on methods to detect isoattenueted tumor [39]. The quantitative analysis at triphasic MDCT increases tumor detection with respect to visual analysis, showing a higher sensitivity in all phases, even for small PDAs isodense to the pancreatic parenchyma upstream to the tumor [39].

Technique - Many CT protocols for pancreatic enhancement and pancreatic tumor staging are described in the literature. In patients with suspected pancreatic tumor, the maiority of standard CT protocols [40-43] involves non-contrast study followed by pancreatic parenchymal phase (PPP) and portal venous phase (PVP) and delayed phase (DP), after the administration of intravenous contrast material.

An arterial phase may be performed if a hypervascular pancreatic lesion such as a neuroendocrine tumor is suspected, while PPP (typically 40-45 seconds after contrast injection) allows maximal differentiation between the normal parenchyma and the hypodense pancreatic lesions, becoming the most sensitive phase for the evaluation of pancreatic parenchyma (e.g. adenocarcinoma) [36,40]. PVP (70 seconds after contrast injection) is optimal for detecting liver metastases.

Nevertheless, multiphase CT exposes patient to a high radiation dosse. Recently, the split-bolus CT protocol has been proposed for the detection and staging of pancreatic cancer [44].

Split-bolus MDCT technique, combining arterial phase (AP) and PVP, allows an optimal pancreatic enhancement to detect normal pancreatic parenchyma and to maximize the difference in attenuation between the tumor and the background pancreatic parenchyma with a better tumor conspicuity, provides optimal synchronous arterial and mesenteric venous opacification evaluating potential tumor resecability, and reduces radiation dose [44-46]. In addition, Split-bolus allows lymph nodes assessment, detection and characterization of the focal liver lesion [45].

In Figure 1 is reported a schematic view of Split-bolus MDCT protocol in a patient weighting 75 Kg.

MRI

MRI, including morfologic and functional sequences, has become widely used in the diagnosis of pancreatic pathologies because of its very high soft-tissue contrast resolution, with an accuracy in the detection and staging of adenocarcinoma of 90%-100% [47]; MR cholangiopancreatography (MRCP) permits the evaluation of pancreatic ductal system anatomy and abnormalities and can be used to depict relationship between cystic lesions and pancreatic duct [48,49]. MRI is used as a problem-solving tool for diagnosis and during follow-up in patients with cystic pancreatic tumors [50].

Furthermore, diffusion-weighted imaging (DWI), almost become part of the MRI protocol, may provide additional information about a wide variety of solid and cystic lesions of the pancreas and can help radiologists, especially to detect solid pancreatic tumors with a high cellularity or fibrosis, which show a low ADC (apparent diffusion coefficient) values [48], and potentially to distinguish focal pancreatitis from adenocarcinoma, as reported in literature [52].

MRI can be performed with scanning at 1.5-T or 3-T: studies comparing 1.5-T and 3-T abdominal MRI suggest that 3-T does not offer substantial improvement in image quality for unenhanced

images; however, the signal-noise ratio (SNR) of contrast-enhanced images is thought to be superior at 3 T [52-59].

Technique – A complete evaluation of the pancreas and the pancreato-biliary ductal system includes a multiparametric-MRI (mp-MRI) T2-weighted (T2W) and diffusion-weighted imaging (DWI), as well as contrast-enhanced MRI) and cholangio-pancreatography (MRCP) pulse sequences (HASTE) using the following sequences: axial T1-weighted gradient-echo, with and without fat saturation, using breath-hold or gated respirations, axial and coronal T2W images with and without fat saturation, either fast spin echo (FSE) or turbo spin echo (TSE), T1W breath-hold fat-suppressed 3D gradient-echo images before and after gadolinium (Gd-DTPA) administration and spin echo EPI single shot (DWI) with b value 0, 800, 1000 and ADC maps reconstruction. Contrast-enhanced MRI includes multiphase (PPP, PVP and DP) study after intravenous administration of Gd-DTPA.

The MRCP sequences can be obtained by 3-dimensional (3D) acquisition that produces high resolution images of the pancreato-biliary ductal system. Pineapple and blueberry juice have been used as oral contrast agents to reduce the signal from the overlying stomach and duodenum.

Secretin MR cholangiopancreatography (S-MRCP) sequence, which entails administration of secretin to stimulate the exocrine function of the pancreas, have been developed for a more complete assessment of pancreatic ducts and glandular function, useful in assessment of complex ductal anomalies and to quantitatively assess the exocrine function of the pancreas [49].

PET/CT

Nuclear medicine is able to provide a functional imaging of pancreatic tumours of different histology and its contribution is of pivotal importance to better diagnose and follow up pancreatic lesions.

Many papers investigated the diagnostic ability of pancreatic cancer of Positron Emission Tomography (PET) with 2-deoxy-[^{18}F]fluoro-D-glucose (^{18}FDG), a radiocompound labelled with ^{18}Fluorine (^{18}F) that uses glycolytic pathways and has an uptake mechanism in tumour cells depending on the increased number of functional glucose transporters and glycolytic enzymes [61]. The wide diffusion of hybrid systems, combining nuclear medicine (SPECT and PET) and radiology devices (CT, MRI) mounted on the same gantry to obtain co-registered and fused functional and anatomical images, improves diagnostic results in clinical practice [60,61]. In a recent meta-analysis the sensitivity and specificity of 18FDG-PET to confirm suspected pancreatic cancer resulted up to 95% and 100%, respectively [61].

A further promising radiopharmaceutical has been proposed to image pancreatic cancer, the thymidine analogue 3-deoxy-3′-[18F]fluorothymidine (^{18}FLT) [62]. This radiocompound allows to visualize proliferating lesions and it has been shown that it selectively accumulates in malignant tumours of the pancreas [63], but its use is still limited.

Furthermore pancreas is a site of neuroendocrine tumours (NET). Pancreatic NET are less frequent than endocrine gastrointestinal tumours and, although generally asymptomatic, they may cause hypersecretion of several hormones (gastrin, insulin, glucagon, vasoactive intestinal peptide) and usually over-express somatostatin receptors (SSR) 1–5 [64-67].

Among positron emitting radiopharmaceuticals ^{18}FDG does not represent the option of choice because it better detects highly metabolic undifferentiated tumours, while other radiotracers such as ^{18}F-DOPA (3,4-dihydroxy-L-phenylalanine labelled with ^{18}F) and peptides labelled with ^{68}Ga provide better results [68]. NET are avid of ^{18}F-DOPA because they derive from cells belonging to the amine precursor uptake and decarboxylation (APUD) cell system and therefore show a high L-DOPA decarboxylase activity [69] while ^{68}Ga-DOTA peptides are radiolabelled somatostatin analogues binding to somatostain receptors (SR) that are over-expressed on NET tumour cell surface (70).

The most known PET tracer for SR imaging are [^{68}Ga-DOTA0 ,Tyr3]octreotate (^{68}Ga-DOTATATE), [^{68}Ga-DOTA0,Tyr3]octreotide (^{68}Ga-DOTATOC) and 1,4,7,10-tetraazacyclododecane-1,4,7,10-tetraacetic acid]-1-Nal3-octreotide (^{68}Ga-DOTANOC) and they are useful to evaluate SR expression in order to treat the patients with□□-emitting labelled somatostatin analogues [60,70], such as radiocompounds labelled by ^{90}Yttrium (^{90}Y) and ^{177}Lutetium (^{177}Lu).

Despite the clinical relevance of ^{68}Ga-labelled radiocompounds also due to the high spatial resolution of PET scan comparing with SPECT, the □-emitting somatostatin analogues maintain a certain role. ^{111}In-DTPA-octreotide is commercially available and is the most commonly used agent for SR imaging [70,71]. It shares with positron-emitting radiopharmaceuticals the clinical indications including the diagnosis of primary and metastatic NET, the staging and the follow-up of patients and the selection of subjects with inoperable and/or metastatic tumours candidates to peptide receptor radionuclide therapy.

SOLID LESIONS

Pancreatic ductal adenocarcinoma

Pancreatic ductal adenocarcinoma (PDA), 85%-95% of all pancreatic solid pancreatic malignant neoplasms, represent the fourth leading cause to cancer-related deaths and affects men more frequently between 60-80 years of age [1-4]. PDA is located in the pancreatic head 60%-70%, less commonly in the body (10%-20%) and 5%-10% in the tail [1-3]. Postoperative survival rate at 5-year is of 20% [1,3], furthermore the cancer is resectable at diagnosis in only about 20-15% of cases [49]. CA 19.9 can be elevated, but it is useful during follow-up because its rise up precedes imaging manifestation of relapse [49].

On PPP of the conventional bi- or triphasic CT and on mixed (PPP/PVP) phase of Split-bolus MDCT protocol, most tumors are hynomogeneous hypoattenuating after intravenous contrast medium injection (Figure 2); the 10% of cases may be isoattenuating [1,39,37]: mass effect,

abnormal contour of the pancreas, ductal obstruction with “double duct sign”, and vascular invasion (vessel deformity, thrombosis, and development of collateral vessels) are indirect signs of pancreatic cancer [1,2]. Rarely (8% of cases) can be see cystic-necrotic degeneration [72].

At MRI PDA show low signal intensity on T1w images and appears hypovascular than the normal pancreas after paramagnetic contrast medium administration; sometimes exhibit delayed enhancement [48]. On dynamic images the PPP allows the greatest attenuation difference between cancer and normal pancreatic parenchyma; T2w images shows less tumor conspicuity, furthermore is useful to emphasize secondary signs as upstream pancreatic ductal dilatation.

In addition to morphological and multiphasic contrast-enhanced imaging, functional informations on cellularity provided by DWI further improve MRI diagnostic accuracy. Since malignant tumors are characterized by limited diffusion due to fibrosis and hypercellularity, DWI and apparent diffusion coefficient (ADC) values provide a high degree of contrast between PA and normal pancreatic parenchyma: pancreatic tumours have increased signal intensity on diffusion weighted images with high b values ($b > 500$ sec/mm^2) and relatively low ADC values [48]. In addition, DWI may be helpful in the earlier detection of cancer and lymph nodes and/or liver metastases [48,73-75]. Instead, it is difficult to differentiate between mass-forming focal pancreatitis and poorly differentiated PDA [48].

Representative case of PDA evaluated by mp-MRI is reported in Figure 3.

Endoscopic US, specially used to perform biopsies, plays a key role in the detection and staging of small tumors (up to 0.2 cm) and clarify equivocal cases at CT or MRI showing an ill-defined, heterogeneous hypoechoic mass [1].

On ^{18}FDG PET evaluation PDA generally shows intense focal FDG uptake due to enhanced glucose metabolism. ^{18}FDG PET is potentially useful to detection small metastases that can be underestimate at MDCT and MRI.

Pancreatic neuroendocrine tumor

Pancreatic neuroendocrine tumors (NET) represent about 1%-5% of all pancreatic tumors and occur sporadically in patients in their third to sixth decades [76]. In some cases, association with multiple endocrine neoplasia type 1 (MEN1), neurofibromatosis type 1, von Hippel-Lindau syndrome and tuberous sclerosis can been observed.

The NET often shows a homogeneous or heterogeneous hyperenhancing pattern at the early stage in CEUS, depending on the amount of the stroma within the lesion [77-79].

On AP or PPP of the conventional bi- or triphasic MDCT and in mixed (PPP/PVP) phase of Split-bolus MDCT protocol, the NET appears hyperattenueted in comparison to adjacent pancreatic parenchyma. Small NET (< 2 cm) shows typical homogeneous intense enhancement during the arterial phase whereas greatest lesions show heterogeneous enhancement, a finding due to areas of cystic degeneration, necrosis, fibrosis and calcification [1,80,81].

NET are usually more conspicuous on T1-weighted images; the presence of cystic component (necrosis or cystic degeneration) are typically hyperintense on T2 MRI. Malignant NET may show high signal intensity on DWI with high b values and low ADC values due to restriction by dense tumor cellularity; benign small NET can have a relatively high ADC values [48].

As previously reported pancreatic NET can be successfully evaluated by imaging with somatostatin analogues labeled by □□□and □-emitting radiopharmaceuticals, while ^{18}FDG can be used to evaluate more aggressive and less differentiated tumors.

Represented cases of functional and non-functional NET (US, Split-bolus MDTC, mp-MRI) are reported in Figure 4-6.

Solid pseudopapillary tumor

Solid pseudopapillary tumor (SPT), most commonly localized in the pancreatic tail and in young females, constitute approximately 1%-2% of all pancreatic neoplasms [82,83], with an excellent

prognosis following complete resection. Rarely malignant degeneration can occur, just as in liver and peritoneum metastases [1,84].

On CT, SPT usually can be seen as a large well-encapsulated mass with cystic, solid or hemorrhagic components [1,79,85] that displace surrounding structures without obstruction of the bile duct or pancreatic duct; peripheral calcification can be seen in 30% of cases [83]. The pseudocapsule (compressed pancreatic tissue and fibrosis) is an important feature to distinguish these neoplasms.

After contrast medium injection, the SPT shows peripheral slow early heterogeneous enhancement during arterial phase of solid component with central cystic spaces [82].

MRI demonstrates the small tumors, most frequently functioning tumors, as solid and homogeneous and larger tumors, most frequently nonfunctioning tumors, as heterogeneous mass with an heterogeneous signal intensity on T1- and T2W images. The degree of diffusion and ADC values are dependent to cystic or hemorrhagic fluid; solid component usually can show relatively low ADC values [48].

Most of the papers on ^{18}FDG PET in pancreatic tumours concern PDA, but a recent interesting paper [86] retrospectively reviewed the records of 11 subjects with SPT and 46 patients with pancreatic ductal adenocarcinoma, showing high ^{18}FDG uptake also in SPT and concluding that this rare tumour should be considered when a solid pancreatic mass with increased ^{18}FDG uptake is revealed at PET/CT scan.

Pancreatoblastoma

Pancreatoblastoma, the most common pancreatic tumor in young children (mean 5 years), is rare in adults (< 1% of all pancreatic tumors) [48,87]. Pancreatoblastoma is typically an asymptomatic, well-encapsulated and heterogeneous large mass; it coexists with an increase of serum alpha-fetoprotein level in 25%-33% of cases [1]. Metastases are rare.

This tumor is heterogeneous with hypoechoic cystic spaces and hyperechoic internal septa at US evaluation [88].

On MRI pancreatoblastoma shows intermediate signal intensity at T1- and T2-weighted with small hyperintense areas in T2. The solid component exhibits rapid enhancement during arterial phase and wash-out in delayed phase after contrast medium administration and restricted diffusion due to dense cellularity on DWI [82].

Pancreatic lymphoma

Primary pancreatic lymphoma, most frequent in immunocompromised patients, constitutes 0.5% of pancreatic tumors and is most commonly a B-cell subtype of non-Hodgkin lymphoma [1,89]. More common is a secondary lymphoma as result of direct extension from peripancreatic lymphadenopathy. Clinical presentation of primary pancreatic lymphoma is nonspecific; the most common findings were abdominal pain and weight loss.

Pancreatic lymphoma occurs in a focal well-circumscribed form (uniform low attenuation and minimal enhancement at CT; hypointensity on T1W images and intermediate signal intensity on T2W images and slight contrast enhancement at MRI) and a diffuse pattern (diffuse enlargement and hypointensity on T1- and T2 w images and moderate homogeneous enhancement at MRI) that can simulate the appearance of acute pancreatitis [1,90]. Imaging findings can show encasement of peripancreatic vessels [91].

Imaging findings are not specific in the differentiation of pancreatic lymphoma and pancreatic cancer, but a bulky homogeneous tumoral mass without alteration of Wirsung's duct should suggest the diagnosis [92].

CYSTIC LESIONS

Cystic lesions represents 10%-15% of all pancreatic tumors. An important distinction among neoplastic cysts is the categorization into four subtypes unilocular, macrocystic: multilocular, microcystic and cystic with a solid component and in mucinous versus nonmucinous. The first aim of imaging is to characterize cystic neoplasms, to confirm or to exclude a communication between

the cystic lesion and the pancreatic duct and to distinguish these from pseudocysts (encapsulated fluid collections without necrosis after 4 week from onset of acute pancreatitis) [93].

When small (< 3 cm) cysts are represented by unilocular lesions, well defined and without internal septa, calcification or internal soft-tissues nodules, it is suggested a close surveillance with serial imaging at 6-months intervals for the first year and annual follow-up for next three years.

Usually imaging shows a cystic mass with a thick wall that exhibits mild enhancement after intravenous contrast injection.

Serous cystadenoma

Serous cystadenomas are benign cystic tumors (20% of all pancreatic cystic neoplasms), typically diagnosed incidentally in asymptomatic patients, most frequently in older women, which do not require surgical excision. The lesion appears as a cluster of cysts well-defined (without visible communication with pancreatic duct) with a high signal intensity on MRI T2W images (Figure 7-8), with a thin fibrous septa that can show delayed enhancement after contrast medium administration. Two subtypes of lesions are known: microcystic serous cystadenomas, composed of multiple cysts (each < 2 cm), separated by fibrous septa originated from a central calcified scar, and macrocystic serous cystadenomas, uncommon, composed of large cysts (1-8 cm). A central calcified scar is highly specific and best demonstrated at CT [48]. When associated with von Hippel–Lindau (VHL) disease, multifocal cystic lesions can involve the pancreatic gland diffusely [93].

The features in DWI and ADC are depending on the amount of fibrous septa or fluid in the lesion; occasionally serous cystadenomas with fibrous septa can show relatively higher signal intensity on DWI and lower ADC values compared with non-neoplastic cysts. On the bases of DWI the differential diagnosis between these lesions and non-neoplastic cysts is difficult [48].

Mucinous cystic neoplasm (mucinous cystadenoma/cystadenocarcinoma)

Mucinous cystic neoplasm (10% of all pancreatic cystic neoplasms), are most frequently diagnosed in women (80%) in their sixth decade of life [86,94] and are preferentially localized in body and pancreatic tail without communication with pancreatic duct [unlike intraductal papillary mucinous neoplasms (IPMNs)].

The lesion appears as a multilocular or unilocular or midly septated cysts well-defined, usually > 2 cm (Figure 9). In relation to the degree of hemorrhage or the amount of protein in the mucoid cysts, CT shows different levels of attenuation [93] and the lesion may be hyperintense on T1-weighted images.

Imaging is unable to distinguish cystadenoma from cystadenocarcinoma, furthermore intracystic enhancing soft tissues, invasion of adjacent organs and vascular invasion are suspicious for malignancy, as metastatic disease too. The rare (16%) presence of peripheral eggshell calcifications has a highly predictive value for malignancy. DWI will not distinguish between mucinous cystic neoplasm and non-neoplastic mucinous cystic neoplasm due to the relatively high ADC values [48].

Intraductal papillary mucinous tumor of the pancreas

IPMNs of the pancreas represent 20% of cystic pancreatic lesions and occur more frequently in elderly men [83,91]. The histopathologic characteristics of IPMNs are papillary growth and hyperproduction of mucina which causes dilatation of the main pancreatic duct, its branches or both [48,49,94,95]. The characteristic imaging feature of IPMNs is the communication of lesion with pancreatic ducts, demonstrate on MRI [48], useful to differentiate them from mucinous cystadenoma (Figure 10).

IPMNs may frequently be multifocal and may have benign or malignant behavior on the basis of the degree of dysplasia; when it affects the main duct, the lesion is more likely to be malignant.

The features suggestive of invasive carcinoma are the large size of the mass (> 3 cm), presence of mural nodules, dilatation of the main pancreatic duct > 1 cm and multifocal involvement [49].

DWI does not allow a differential diagnosis because IPMNs usually show an high ADC value even in cases of carcinomas in situ [48].

METASTASES

Pancreatic metastases occur in 2%-5% of all malignant neoplasms and originate most frequently from renal cell carcinoma, lung carcinoma, breast carcinoma, colorectal carcinoma, ovarian carcinoma and melanoma [96]. Imaging features are non-specific: metastases can be solid or cystic, hypo- or hyper-vascular depending on primary tumor and can be solitary (50%-70%), multifocal or diffuse [1,96-99] (Figure 11-12).

IMAGING AFTER SURGERY

The knowledge of the type of surgical procedures (Whipple procedure, distal pancreatectomy, central pancreatectomy or total pancreatectomy) and the normal post-operative appearances are essential for an accurate evaluation of the complications and recurrent disease.

Several imaging techniques can be used after pancreatic surgery. US plays a limited role in the early post-operative period useful only for the peritoneal fluid detection.

In the immediate post-operative period the most common findings are fluid peritoneal or peri-pancreatic collections, increased density of the mesenteric fat tissue, reactive adenopathy and pneumobilia; early and late surgical complications as anastomosis leakage, pancreatico-jejunal fistula, peritonitis, abscess, aneurysms, anastomotic stenosis, perianastomotic ulcers, biloma and intra-abdominal bleeding, are better detected on CT imaging.

CT represents the first choice for the evaluation of tumor recurrence and for the assessment of lymph nodes and liver metastasis [99].

MRI may be used as alternative imaging modality to CT or in cases of inconclusive CT findings; furthermore, MRI combined with functional DWI potentially provides helpulf information about locally recurrent disease.

Also ^{18}FDG PET is useful to detect recurrent disease after surgery, but PET scan has to be performed for some months after surgical treatment to avoid unspecific uptake of the radiocompound due to inflammatory reaction after therapy (Figure 13).

CONCLUSION

In order to a prompt and accurate diagnosis and appropriate management of pancreatic lesions, it is crucial for radiologists to know the key findings of the most frequent tumors of the pancreas and the current role of imaging modalities.

A multimodality approach is often helpful. If MDCT is the preferred initial imaging modality in patients with clinical suspicion for pancreatic cancer, multiparametric MRI provides essential information for the detection and characterization of a wide variety of pancreatic lesions and can be used as a problem-solving tool at diagnosis and during follow-up.

REFERENCES

1. Low G, Panu A, Millo N, Leen E. Multimodality imaging of neoplastic and nonneoplastic solid lesions of the pancreas. Radiographics 2011;31(4):993-1015.

2. Ros PR, Mortelé KJ. Imaging features of pancreatic neoplasms. JBR-BTR 2001;84(6):239–249.

3. Pavan Tummala, Omer Junaidi, Banke Agarwal. Imaging of pancreatic cancer: An overview. J Gastrointest Oncol 2011; 2(3): 168-174.

4. Mujica VR, Barkin JS, Go VL. Acute pancreatitis secondary to pancreatic carcinoma. Study Group Participants. Pancreas 2000;21(4):329-32.

5. Porta M, Fabregat X, Malats N, Guarner L, Carrato A, de Miguel A, Ruiz L, Jariod M, Costafreda S, Coll S, Alguacil J, Corominas JM, Solà R, Salas A, Real FX. Exocrine pancreatic cancer: symptoms at presentation and their relation to tumour site and stage. Clin Transl Oncol 2005;7(5):189-197.

6. Khoranaa AA, Fine RL. Pancreatic cancer and thromboembolic disease. The Lancet Oncology 2004;5(11):655-663.

7. Pinzon R, Drewinko B, Trujillo JM, Guinee V, Giacco G. Pancreatic carcinoma and Trousseau's syndrome: experience at a large cancer center. J Clin Oncol 1986;4(4):509-14.

8. Gorovoy IR, McSorley J, Gorovoy JB. Pancreatic panniculitis secondary to acinar cell carcinoma of the pancreas. Cutis 2013;91(4):186-90.

9. Ulla JL, Garcia-Doval I, Posada C, Soto S, Alvarez C, Ledo L, Vazquez-Astray E. Plantar keratoderma as a presenting sign of pancreatic adenocarcinoma. J Clin Ultrasound. 2008;36(2):108-9. Werner G, Herzig S. Paraneoplastic Syndromes in Pancreatic Cancer. Pancreatic Cancer 2010, pp 651-673.

10. Ito T, Igarashi H, Jensen RT. Pancreatic neuroendocrine tumors: clinical features, diagnosis and medical treatment: advances. Best Pract Res Clin Gastroenterol 2012;26(6):737-53.

11. Metz DC, Jensen RT. Gastrointestinal neuroendocrine tumors; pancreatic endocrine tumors. Gastroenterology 2008;135:1469-1492.

12. Grant CS. Insulinoma. Best Pract Res Clin Gastroenterol 2005;19:783-798.

13. Gibril F, Schumann M, Pace A, Jensen RT. Multiple endocrine neoplasia type 1 and Zollinger-Ellison syndrome. A prospective study of 107 cases and comparison with 1009 patients from the literature. Medicine (Baltimore) 2004;83:43-83.

14. Roy PK, Venzon DJ, Shojamanesh H, Abou-Saif A, Peghini P, Doppman JL, et al. Zollinger-Ellison syndrome: clinical presentation in 261 patients. Medicine (Baltimore) 2000;79:379-411.

15. Jensen RT, Norton JA. Endocrine tumors of the Pancreas and Gastrointestinal Tract. In: Feldman M, Friedman LS, Brandt LJ, editors. Sleisenger and Fordtran's Gastrointestinal and Liver Disease. Philadelphia: Saunders; 2010. pp. 491-522.

16. Jensen RT, Niederle B, Mitry E, Ramage JK, Steinmuller T, Lewington V, Scarpa A, Sundin A, Perren A, Gross D, O'Connor JM, Pauwels S, Kloppel G; Frascati Consensus Conference; European Neuroendocrine Tumor Society. Gastrinoma (duodenal and pancreatic) Neuroendocrinology 2006;84:173-182.

17. Nikou GC, Toubanakis C, Nikolaou P, Giannatou E, Safioleas M, Mallas E, Polyzos A. VIPomas: an update in diagnosis and management in a series of 11 patients. Hepatogastroenterology 2005;52:1259-1265.

18. Eldor R, Glaser B, Fraenkel M, Doviner V, Salmon A, Gross DJ. Glucagonoma and the glucagonoma syndrome - cumulative experience with an elusive endocrine tumour. Clin Endocrinol (Oxf) 2011;74:593–598.

19. Nesi G, Marcucci T, Rubio CA, Brandi ML, Tonelli F. Somatostatinoma: Clinico-pathological features of three cases and literature reviewed. J Gastroenterol Hepatol 2008;23:521–526.

20. Kuo SC, Gananadha S, Scarlett CJ, Gill A, Smith RC. Sporadic pancreatic polypeptide secreting tumors (PPomas) of the pancreas. World J Surg 2008;32(8):1815-22.

21. Pinto A, Reginelli A, Cagini L, Coppolino F, Stabile Ianora AA, Bracale R, Giganti M, Romano L. Accuracy of ultrasonography in the diagnosis of acute calculous cholecystitis: review of the literature. Crit Ultrasound J. 2013 Jul 15;5 Suppl 1:S11.

22. Cagini L, Gravante S, Malaspina CM, Cesarano E, Giganti M, Rebonato A, Fonio P, Scialpi M. Contrast enhanced ultrasound (CEUS) in blunt abdominal trauma. Crit Ultrasound J 2013; 5(1):S9.

23. Karlson BM, Ekbom A, Lindgren PG, Kalskogg V, Rastad J. Abdominal US for diagnosis of pancreatic tumor: prospective cohort analysis. Radiology 1999;213:107-11.

24. Rickes S, Unkrodt K, Neye H, Ocran KW, Wermke W. Differentiation of pancreatic tumours by conventional ultrasound, unenhanced and echo-enhanced power Doppler sonography. Scand J Gastroenterol 2002;37:1313-1320.

25. Wiersema MJ. Accuracy of endoscopic ultrasound in diagnosing and staging pancreatic carcinoma. Pancreatology 2001;1:625-635.

26. Piscaglia F, Nolsoe C, Dietrich CF et al. The EFSUMB guidelines and recommendations on the clinical practice of contrast enhanced ultrasound (CEUS): update 2011 on non-hepatic applications. Ultraschall in Med 2012;5:33-59.

27. Kobayashi A, Yamaguchi T, Ishihara T, Tadenuma H, Nakamura K, Saisho H. Evaluation of vascular signal in pancreatic ductal carcinoma using contrast-enhanced ultrasonography: effect of systemic chemotherapy. Gut 2005; 54:1047.

28. Scialpi M, Midiri M, Bartolotta TV, Cazzolla MP, Rotondo A, Resta MC, Lagalla R, Cardinale AE. Pancreatic carcinoma versus chronic focal pancreatitis: contrast-enhanced power Doppler ultrasonography findings. Abdom Imaging 2005;30(2):222-227.

29. D'Onofrio M, Barbi E, Dietrich CF, Kitano M, Numata K, Sofuni A, Principe F, Gallotti A, Zamboni GA, Mucelli RP. Pancreatic multicenter ultrasound study (PAMUS). Eur J Radiol 2012;81(4):630-638.

30. Ardelean M, ªirli R, Sporea I, Bota S, Martie A, Popescu A, Dãnila M, Timar B, Buzas R, Lighezan D. Contrast enhanced ultrasound in the pathology of the pancreas - a monocentric experience. Med Ultrason 2014;16(4):325-331.

31. Grossjohann HS. Contrast-enhanced ultrasound for diagnosing, staging and assessment of operability of pancreatic cancer. Dan Med J 2012;59(12):B4536.

32. Recaldini C, Carpafiello G, Bertolotti E, Angeretti AG, Fugazzola C. Contrast-enhanced ultrasonographic findings in pancreatic tumors. Int J Med Sci 2008; 5:203-208.

33. Ripolles T, Martinez MJ, Lopez E, Castello I, Delgado F. Contrast-enhanced ultrasound in the staging of acute pancreatitis. Eur Radiol 2010; 20: 2518-2523.

34. Ichikawa T, Haradome H, Hachiya J, Nitatori T, Ohtomo K, Kinoshita T, Araki T. Pancreatic ductal adenocarcinoma: preoperative assessment with helical CT versus dynamic MR imaging. Radiology 1997;202:655-62.

35. Fletcher JG, Wiersema MJ, Farrell MA, Fidler JL, Burgart LJ, Koyama T, Johnson CD, Stephens DH, Ward EM, Harmsen WS. Pancreatic malignancy: value of arterial, pancreatic, and hepatic phase imaging with multi-detector row CT. Radiology 2003;229:81-90.

36. Brennan DD, Zamboni GA, Raptopoulos VD, Kruskal JB. Comprehensive preoperative assessment of pancreatic adenocarcinoma with 64-section volumetric CT. RadioGraphics 2007;27(6):1653-1666.

37. Prokesch RW, Chow LC, Beaulieu CF, Bammer R, Jeffrey RB Jr. Isoattenuating pancreatic adenocarcinoma at multi-detector row CT: secondary signs. Radiology 2002;224:764-768.

38. Scialpi M, Cagini L, Pierotti L, De Santis F, Pusiol T, Piscioli I, Magli M, D'Andrea A, Brunese L, Rotondo A. Detection of small (≤ 2 cm) pancreatic adenocarcinoma and surrounding

parenchyma: correlations between enhancement patterns at triphasic MDCT and histologic features. BMC Gastroenterol 2014;21;14-16.

39. McNulty NJ, Francis IR, Platt JF, Cohan RH, Korobkin M, Gebremariam A. Multi-detector row helical CT of the pancreas: effect of contrast-enhanced multiphasic imaging on enhancement of the pancreas, peripancreatic vasculature, and pancreatic adenocarcinoma. Radiology 2001; 220:97-102.

40. Hollett MD, Jorgensen MJ, Jeffrey RB Jr. Quantitative evaluation of pancreatic enhancement during dual-phase helical CT. Radiology 1995; 195:359-361.

41. Graf O, Boland GW, Warshaw AL, Fernandez-del-Castillo C, Hahn PF, Mueller PR. Arterial versus portal venous helical CT for revealing pancreatic adenocarcinoma: conspicuity of tumor and critical vascular anatomy. AJR Am J Roentgenol 1997;169:119-123.

42. Kondo H, Kanematsu M, Goshima S, Miyoshi T, Shiratori Y, Onozuka M, Moriyama N, Bae KT. MDCT of the pancreas: optimizing scanning delay with a bolus-tracking technique for pancreatic, peripancreatic vascular, and hepatic contrast enhancement. AJR Am J Roentgenol 2007;188:751-756.

43. Brook OR, Gourtsoyianni S, Brook A, Siewert B, Kent T, Raptopoulos V. Split-bolus spectral Multidetector CT of the Pancreas: Assessment of Radiation Dose and Tumor Conspicuity. Radiology 2013;269:139-148.

44. Scialpi M, Palumbo B, Pierotti L, Gravante S, Piunno A, Rebonato A, D'Andrea A, Reginelli A, Piscioli I, Brunese L, Rotondo A. Detection and characterization of focal liver lesions by Split-bolus multidetector-row CT: diagnostic accuracy and radiation dose in oncologic patients. Anticancer Res 2014; 34(8):4335-4344.

45. Scialpi M, Piscioli I, Magli M, D'Andrea A. Split-bolus spectral multidetector CT of the pancreas: problem solving in the detection of "isoattenuating" pancreatic cancer?. Radiology 2014;270(3):936-937.

46. Handbidge et al. Cancer of the pancreas: the best image for early detection – CT, MRI, PET or US? Can J Gastroenerol 2002;16(2):101-105.

47. Wang Y, Miller FH, Chen ZE, Merrick L, Mortele KJ, Hoff FL, Hammond NA, Yaghmai V, Nikolaidis P. Diffusion-weighted MR imaging of solid and cystic lesions of the pancreas. Radiographics 2011;31(3):47-64.

48. Quencer K, Kambadakone A, Sahani D, Guimaraes ASR. Imaging of the pancreas: part 1. Applied Radiology 2013.

49. Sandrasegaran K, Lin C, Akisik FM, Tann M. State-of-the-Art Pancreatic MRI. AJR Am J Roentgenol 2010;195(1):42-53.

50. Fatthai et al. Pancreatic diffusion-weighted imaging (DWI): comparison between mass-forming focal pancreatitis (FP), pancreatic cancer (PC), and normal pancreas. J Magn Reson Imaging 2009;29(2):350-356.

51. Schmidt GP, Wintersperger B, Graser A, Baur-Melnyk A, Reiser MF, Schoenberg SO. High-resolution whole-body magnetic resonance imaging applications at 1.5 and 3 Tesla: a comparative study. Invest Radiol 2007;42:449-459.

52. Kim SY, Byun JH, Lee SS, Park SH, Jang YJ, Lee MG. Biliary tract depiction in living potential liver donors: intraindividual comparison of MR cholangiography at 3.0 and 1.5 T. Radiology 2010;254:469-478.

53. Koelblinger C, Schima W, Weber M, Mang T, Nemec S, Kulinna-Cosentini C, Bastati N, Ba-Ssalamah A. Gadoxate-enhanced T1-weighted MR cholangiography: comparison of 1.5 T and 3.0 T. Rofo 2009;181:587-592.

54. Ramalho M, Heredia V, Tsurusaki M, Altun E, Semelka RC. Quantitative and qualitative comparison of 1.5 and 3.0 Tesla MRI in patients with chronic liver diseases. J Magn Reson Imaging 2009;29:869-879.

55. Isoda H, Kataoka M, Maetani Y, Kido A, Umeoka S, Tamai K, Koyama T, Nakamoto Y, Miki Y, Saga T, Togashi K. MRCP imaging at 3.0 T vs. 1.5 T: preliminary experience in healthy volunteers. J Magn Reson Imaging 2007; 25:1000-1006.

56. von Falkenhausen MM, Lutterbey G, Morakkabati-Spitz N, Walter O, Gieseke J, Blömer R, Willinek WA, Schild HH, Kuhl CK. High-field-strength MR imaging of the liver at 3.0 T: intraindividual comparative study with MR imaging at 1.5 T. Radiology 2006;241:156-166.

57. Edelman RR, Salanitri G, Brand R, Dunkle E, Ragin A, Li W, Mehta U, Berlin J, Newmark G, Gore R, Patel B, Carillo A, Vu A. Magnetic resonance imaging of the pancreas at 3.0 tesla: qualitative and quantitative comparison with 1.5 Tesla. Invest Radiol 2006; 41:175-180.

58. Goncalves Neto JA, Altun E, Elazzazi M, Vaidean GD, Chaney M, Semelka RC. Enhancement of abdominal organs on hepatic arterial phase: quantitative comparison between 1.5- and 3.0-T magnetic resonance imaging. Magn Reson Imaging 2010; 28:47-55.

59. Palumbo B, Buresta T, Nuvoli S, Spanu A, Schillaci O, Fravolini ML, Palumbo I. SPECT and PET serve as molecular imaging techniques and in vivo biomarkers for brain metastases. Int J Mol Sci 2014;15(6):9878-93.

60. Rijkers AP, Valkema R, Duivenvoorden HJ, van Eijck CH. Usefulness of F-18-fluorodeoxyglucose positron emission tomography to confirm suspected pancreatic cancer: a meta-analysis. Eur J Surg Oncol 2014; 40(7): 794-804.

61. Herrmann K, Erkan M, Dobritz M, Schuster T, Siveke JT, Beer AJ, Wester HJ, Schmid RM, Friess H, Schwaiger M, Kleeff J, Buck AK. Comparison of 3'-deoxy-3'-[^{18}F]fluorothymidine positron emission tomography (FLT PET) and FDG PET/CT for the detection and characterization of pancreatic tumours. Eur J Nucl Med Mol Imaging 2012;39(5):846-51.

62. Herrmann K, Eckel F, Schmidt S, Scheidhauer K, Krause BJ, Kleeff J, Schuster T, Wester HJ, Friess H, Schmid RM, Schwaiger M, Buck AK. In vivo characterization of proliferation for discriminating cancer from pancreatic pseudotumors. J Nucl Med 2008;49:1437-44.

63. Ueberberg B, Tourne H, Redman A, Walz MK, Schmid KW, Mann K, et al. Differential expression of the human somatostatin receptor subtypes sst1 to sst5 in various adrenal tumors and normal adrenal gland. Horm Metab Res 2005;37(12):722-728.

64. Papotti M, Kuma U, Volante M, Pecchiono C, Patel YC. Immunohistochemical detection of somatostatin receptor types 1–5 in medullary carcinoma of the thyroid. Clin Endocrinol 2001;54:641-649.

65. Oda Y, Tanaka Y, Naruse T, Sasanabe R, Tsubamoto M, Funahashi H. Expression of somatostatin receptor and effects of somatostatin analog on pancreatic endocrine tumors. Surg Today 2002;32(8):690-694.

66. Papotti M, Bongiovanni M, Volante M, Allia E, Landolfi S, Helboe L, et al. Expression of somatostatin receptor types 1–5 in 81 cases of gastrointestinal and pancreatic endocrine tumors. A correlative immunohistochemical and reverse-transcriptase polymerase chain reaction analysis. Virchows Arch 2002;440(5):461-475.

67. Ambrosini V, Tomassetti P, Castellucci P, Campana D, Montini G, Rubello D, Nanni C, Rizzello A, Franchi R, Fanti S. Comparison between 68Ga-DOTA-NOC and 18F-DOPA PET for the detection of gastro-entero-pancreatic and lung neuro-endocrine tumours. Eur J Nucl Med Mol Imaging 2008;35(8):1431-1438.

68. Hoegerle S, Altehoefer C, Ghanem N, Koehler G, Waller CF, Scheruebl H, et al. Whole-body 18F dopa PET for detection of gastrointestinal carcinoid tumors. Radiology 2001;220(2):373-380.

69. Kwikkeboom DJ, Kam BL, van Essen M, Teunissen JJ, van Eijck CH, Valkema R, de Jong M, de Herder WW, Krenning EP. Somatostatin-receptor-based imaging and therapy of gastroenteropancreatic neuroendocrine tumors. Endocr Relat Cancer 2010; 17(1):53-73.

70. Tranfaglia C, Cardinali L, Gattucci M, Scialpi M, Ferolla P, Sinzinger H, Palumbo B. (111)In-pentetreotide SPECT/CT in carcinoid tumours: is the role of hybrid systems advantageous in abdominal or thoracic lesions? Hell J Nucl Med 2011;14(3):274-277.

71. Kosmahl M, Pauser U, Anlauf M, Klöppel G. Pancreatic ductal adenocarcinomas with cystic features: neither rare nor uniform. Mod Pathol 2005;18(9):1157-1164.

72. Freelove R, Walling AD. Pancreatic cancer: diagnosis and management. Am Fam Physician 2006;73(3):485-492.

73. Kandpal H, Sharma R, Madhusudhan KS, Kapoor KS. Respiratory-triggered versus breath-hold diffusion-weighted MRI of liver lesions: comparison of image quality and apparent diffusion coefficient values. AJR Am J Roentgenol 2009;192:915-922.

74. Garcea G, Dennison AR, Pattenden CJ, Neal CP, Sutton CD, Berry DP. Survival following curative resection for pancreatic ductal adenocarcinoma: a systematic review of the literature. JOP 2008;9(2): 99-132.

75. Ehehalt F, Saeger HD, Schmidt CM, Grützmann R. Neuroendocrine tumors of the pancreas. Oncologist 2009;14(5):456-467.

76. Kersting S, Roth J, Bunk A. Transabdominal contrast-enhanced ultrasonography of pancreatic cancer. Pancreatology 2011; 11(Suppl.2):20-27.

77. Serra C, Felicani C, Mazzotta E, Piscitelli L, Cipollini ML, Tomassetti P, Pezzilli R, Casadei R, Morselli-Labate AM, Stanghellini V, Corinaldesi R, De Giorgio R. Contrast-enhanced ultrasound in the differential diagnosis of exocrine versus neuroendocrine pancreatic tumors. Pancreas 2013; 42(5):871-877.

78. Fan Z, Li Y, Yan K, Wu W, Yin S, Yang W, Xing B, Li X, Zhang X. Application of contrast-enhanced ultrasound in the diagnosis of solid pancreatic lesions – A comparison of conventional ultrasound and contrast-enhanced CT. Eur J Radiol 2013;82:1385-1390.

79. Rha SE, Jung SE, Lee KH, Ku YM, Byun JY, Lee JM. CT and MR imaging findings of endocrine tumor of the pancreas according to WHO classification. Eur J Radiol 2007;62(3):371-377.

80. Noone TC, Hosey J, Firat Z, Semelka RC. Imaging and localization of islet-cell tumours of the pancreas on CT and MRI. Best Pract Res Clin Endocrinol Metab 2005;19(2):195-211.

81. Klimstra DS, Pitman MB, Hruban RH. An algorithmic approach to the diagnosis of pancreatic neoplasms. Arch Pathol Lab Med 2009;133(3):454-464.

82. Buetow PC, Buck JL, Pantongrag-Brown L, Beck KG, Ros PR, Adair CF. Solid and papillary epithelial neoplasm of the pancreas: imaging-pathologic correlation on 56 cases. Radiology 1996;199(3):707-711.

83. Al-Qahtani S, Gudinchet F, Laswed T, Schnyder P, Schmidt S, Osterheld MC, Alamo L. Solid pseudopapillary tumor of the pancreas in children: typical radiological findings and pathological correlation. Clin Imaging 2010;34(2):152-156.

84. Yao X, Ji Y, Zeng M, Rao S, Yang B. Solid pseudopapillary tumor of the pancreas: cross-sectional imaging and pathologic correlation. Pancreas 2010;39(4):486-491.

85. Kim YI, Kim SK, Paeng JC, Lee HY. Comparison of F-18-FDG PET/CT findings between pancreatic solid pseudopapillary tumor and pancreatic ductal adenocarcinoma. Eur J Radiol 2014;83(1):231-5.

86. Cavallini A, Falconi M, Bortesi L, Crippa S, Barugola G, Butturini G. Pancreatoblastoma in adults: a review of the literature. Pancreatology 2009;9(1– 2):73–80.

87. Chung EM, Travis MD, Conran RM. Pancreatic tumors in children: radiologic-pathologic correlation. RadioGraphics 2006;26(4):1211-1238.

88. Zucca E, Roggero E, Bertoni F, Cavalli F. Primary extranodal non-Hodgkin's lymphomas. I. Gastrointestinal, cutaneous and genitourinary lymphomas. Ann Oncol 1997;8(8):727-737.

89. Nayer H, Weir EG, Sheth S, Ali SZ. Primary pancreatic lymphomas: a cytopathologic analysis of a rare malignancy. Cancer 2004;102(5):315-321.

90. Van Beers B, Lalonde L, Soyer P, Grandin C, Trigaux JP, De Ronde T, Dive C, Pringot J. Dynamic CT in pancreatic lymphoma. J Comput Assist Tomogr 1993; 17:94-97.

91. Elmar M. Merkle1 , Greg N. Bender, Hans-Juergen Brambs. Imaging Findings in Pancreatic Lymphoma. Differential Aspects. AJR Am J Roentgenol 2000;174(3):671-675.

92. Morana G, Guarise A. Cystic tumors of the pancreas. Cancer Imaging (2006) 6, 60–71.

93. Adsay NV. Cystic neoplasia of the pancreas: pathology and biology. J Gastrointest Surg 2008;12(3): 401-404.

94. Basturk O, Coban I, Adsay NV. Pancreatic cysts: pathologic classification, differential diagnosis, and clinical implications. Arch Pathol Lab Med 2009; 133(3):423-438.

95. Tsitouridis I, Diamantopoulou A, Michaelides M, Arvanity M, Papaioannou S. Pancreatic metastases: CT and MRI findings. Diagn Interv Radiol 2010;16(1):45-51.

96. Muranaka T, Teshima K, Honda H, Nanjo T, Hanada K, Oshiumi Y. Computed tomography and histologic appearance of pancreatic metastases from distant sources. Acta Radiol 1989;30(6):615-619.

97. Dicitore, A., Caraglia, M., Gaudenzi, G., (...), Arra, C., Vitale, G. : Type I interferon-mediated pathway interacts with peroxisome proliferator activated receptor-γ (PPAR-γ): At the cross-road of pancreatic cancer cell proliferation. Biochimica et Biophysica Acta - Reviews on Cancer, 2014, 1845 (1), pp. 42-52 DOI: 10.1016/j.bbcan.2013.11.003

98. Klein KA, Stephens DH, Welch TJ. CT characteristics of metastatic disease of the pancreas. RadioGraphics 1998;18(2):369-378.

99. Scialpi M, Scaglione M, Volterrani L, Lupattelli L, Ragozzino A, Romano S, Rotondo A. Imaging evaluation of post pancreatic surgery. Eur J Radiol 2005;53(3):417-24.

TABLE and FIGURES

Table 1 – Pancreatic tumors and tumor-like lesions				
Tumor lesions				**Tumor-like lesions**
Primitive			**Secondary (from)**	Focal pancreatitis
Solid exocrine tumors	**Solid neuroendocrine tumors (NET)**	**Cystic lesions**		Fatty infiltration-replacement
Ductal adenocarcinoma	Insulinoma	Intraductal papillary mucinous neoplasm (IPMN)	Renal cell carcinoma	Pseudocysts
Acinar cell carcinoma	Gastrinoma	Serous cystoadenoma	Lung carcinoma	Intrapancreatic accessory spleen
Pancreatoblastoma	Glucaconoma	Mucinous cystic neoplasm	Breast carcinoma	Hydatid cysts
Solid pseudopapillary neoplasm	Vipoma	True cyst	Colorectal carcinoma	Fibrocystic disease
Pancreatic lymphoma	Pancreatic polypeptide secreting tumors (PPoma)	Cystic variants of solid tumors (e.g. Cystic teratoma, Cystic ductal adenocarcinoma, Cystic NET)	Melanoma	Duplication cysts and retention cysts
Miscellaneous carcinomas	Somatostatinoma		Ovarian cancer	Sarcoidosis
	Non-functioning tumors		Sarcoma	Castleman disease

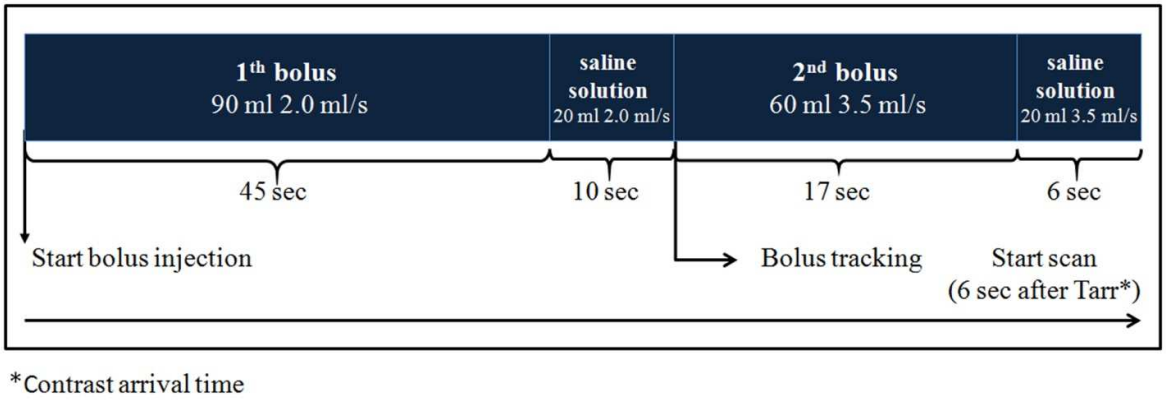

Figure 1. Schematic view of Split-bolus MDCT technique of the chest, abdomen and pelvis shows contrast medium administration splitted into two-bolus injections in adult male (weighed 75 kg). First bolus [at the start of bolus injection (or time zero): 90 ml (1.2 ml/kg) of contrast medium at 2.0 ml/s,

followed by 20 ml of saline solution at same flow rate, is injected to obtain adequate hepatic enhancement during the portal venous phase; second bolus: 60 ml of contrast medium at 3.5 ml/s followed by 20 ml of saline solution at the same flow rate to obtain hepatic arterial phase. CT scanning is started 6-8 sec after to Time of arrival of contrast medium at the aorta (Tarr) determined by bolus tracking technique (raising the threshold value at 500 HU) with a circular region of interest placed in the descending aorta. A single contrast-enhanced acquisition from the pulmonary apex to the pubic symphysis was carried-out, resulting in a simultaneous contrast enhancement of the arterial and venous systems.

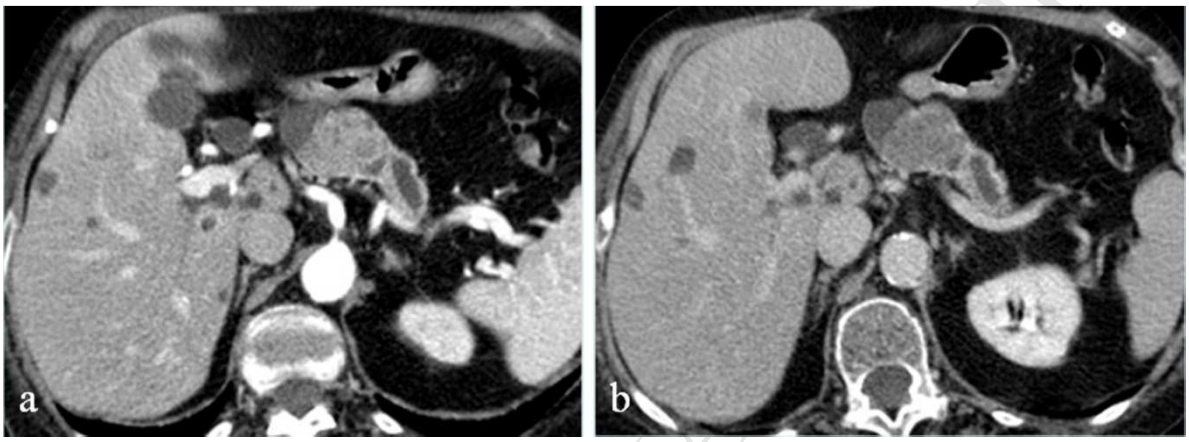

Figure 2. 60-years-old male patient with unresectable pancreatic ductal adenocarcinoma with liver metastasis at initial 64-slice Split-bolus CT protocol. Mixed phase (a) and delayed phase (b) show inhomogeneous lesion in the body of the pancreas. Note dilatation of the Wirsung in the pancreas up-stream to the tumor.

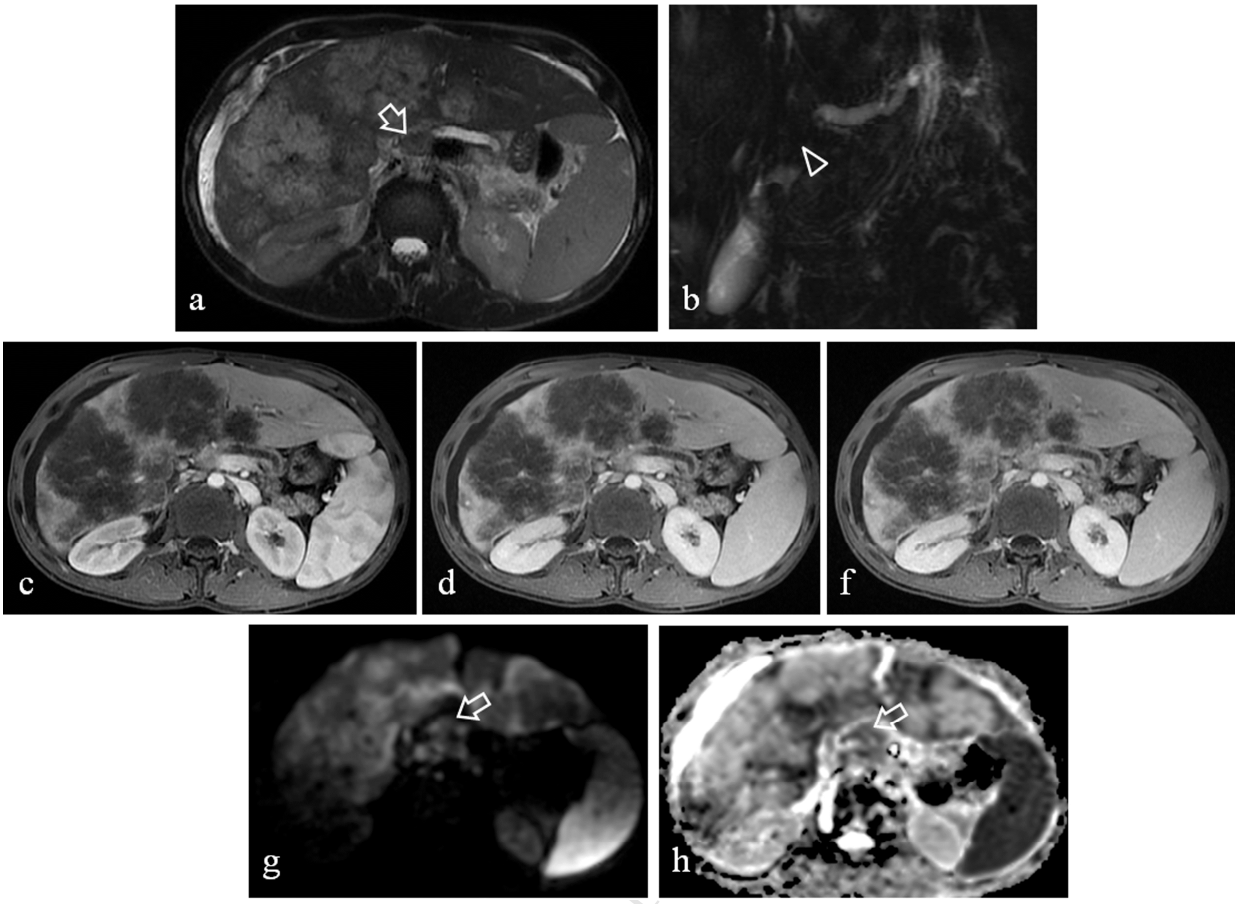

Figure 3. 28-years-old male patient with pancreatic ductal adenocarcinoma with multiple liver metastasis at 3 T mpMRI evaluation. Fat-suppressed T2-weighted images (a) show a slightly inhomogeneous hyperintense lesion (arrow in a) in the body of the pancreas determining dilatation of the Wirsung in the pancreas up-stream to the tumor. MRCP (b) shows the interrupted duct sign (head arrow in b). At multiphase T1W breath-hold fat-suppressed 3D gradient-echo images after intravenous administration of gadolinium (Gd-DTPA)(c-f) the lesion appears inhomogeneous with maximum enhancement on delayed phase (f). On DWI with b=1000 values (g) and ADC map (h) the tumor (arrow in g and h) show restriction of the diffusion of the water molecules.

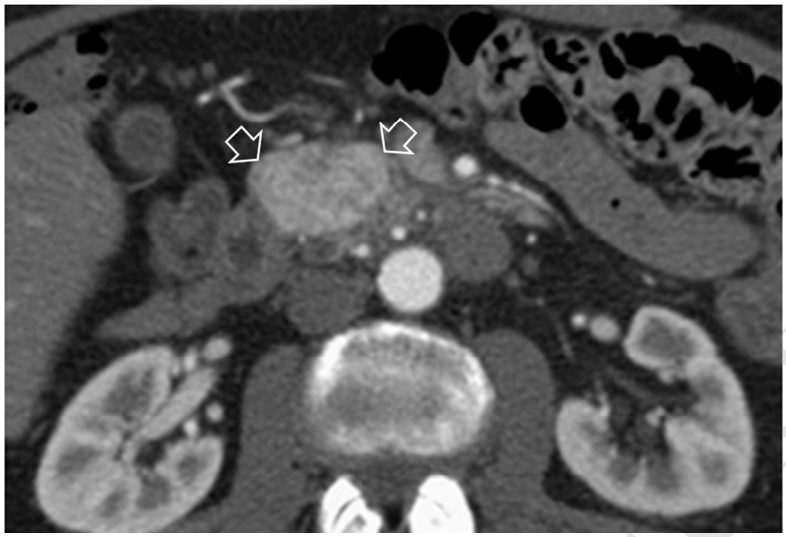

Figure 4. 79-years-old male patient with neuroendocrine pancreatic tumor (NET) on pancreatic at 64-slice CT. Pancreatic parenchymal phase show well defined lesion with intense enhancement at the isthmus of the pancreas.

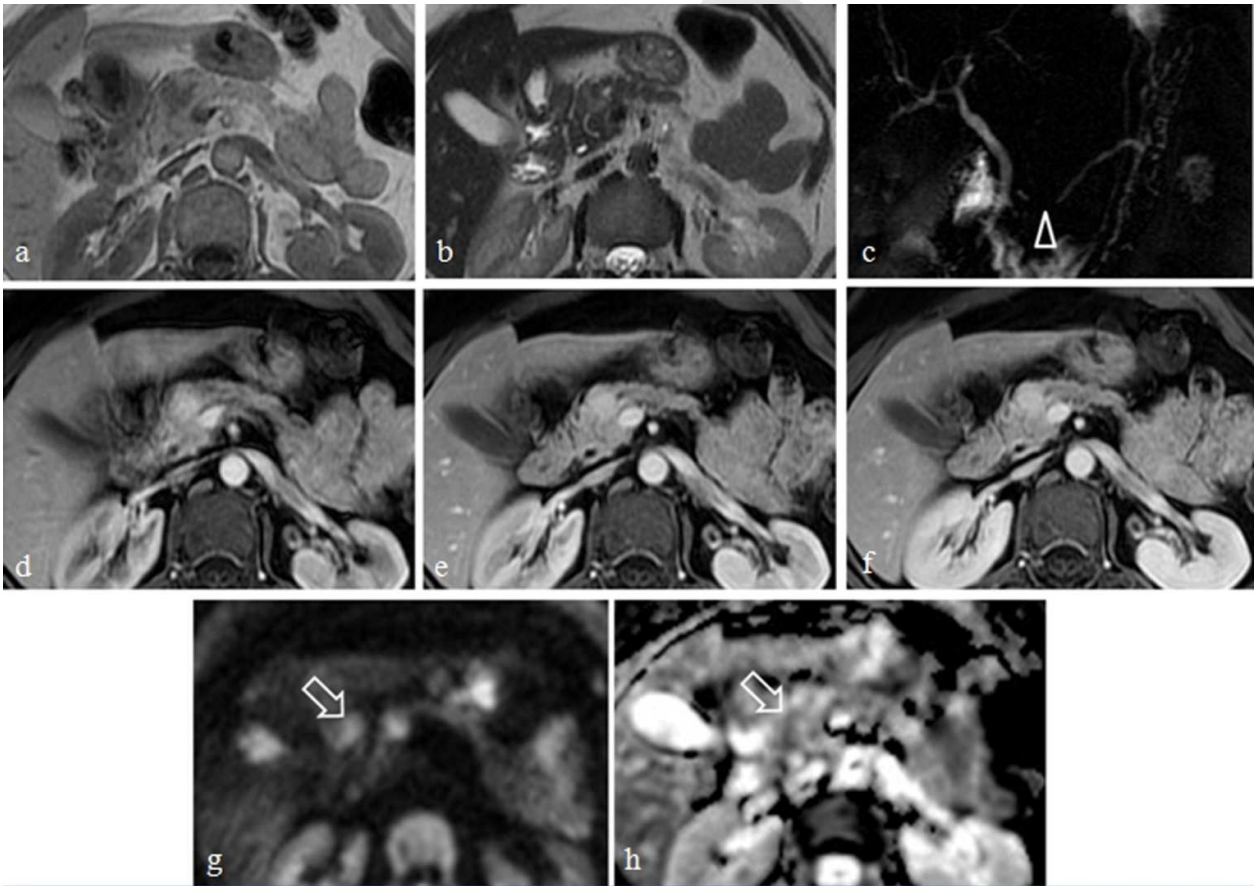

Figure 5. 54-years-old female patient with functioning neuroendocrine pancreatic tumor (NET) at 3 T mpMRI evaluation. The lesion appears hypointense on T1W images (a), slightly hyperintense on T2W images (b). MRCP (c) shows interruption of the Wirsung (head arrow in c). At multiphase

T1W breath-hold fat-suppressed 3D gradient-echo images after intravenous administration of gadolinium (Gd-DTPA) (d-f) the lesion exhibits intense enhancement in arterial phase (arrow in a) which persists during venous and delayed phase (arrow in e and f). On DWI with b=1000 values (g) and ADC map (h) the tumor (arrow in g and h) show restriction of the diffusion of the water molecules.

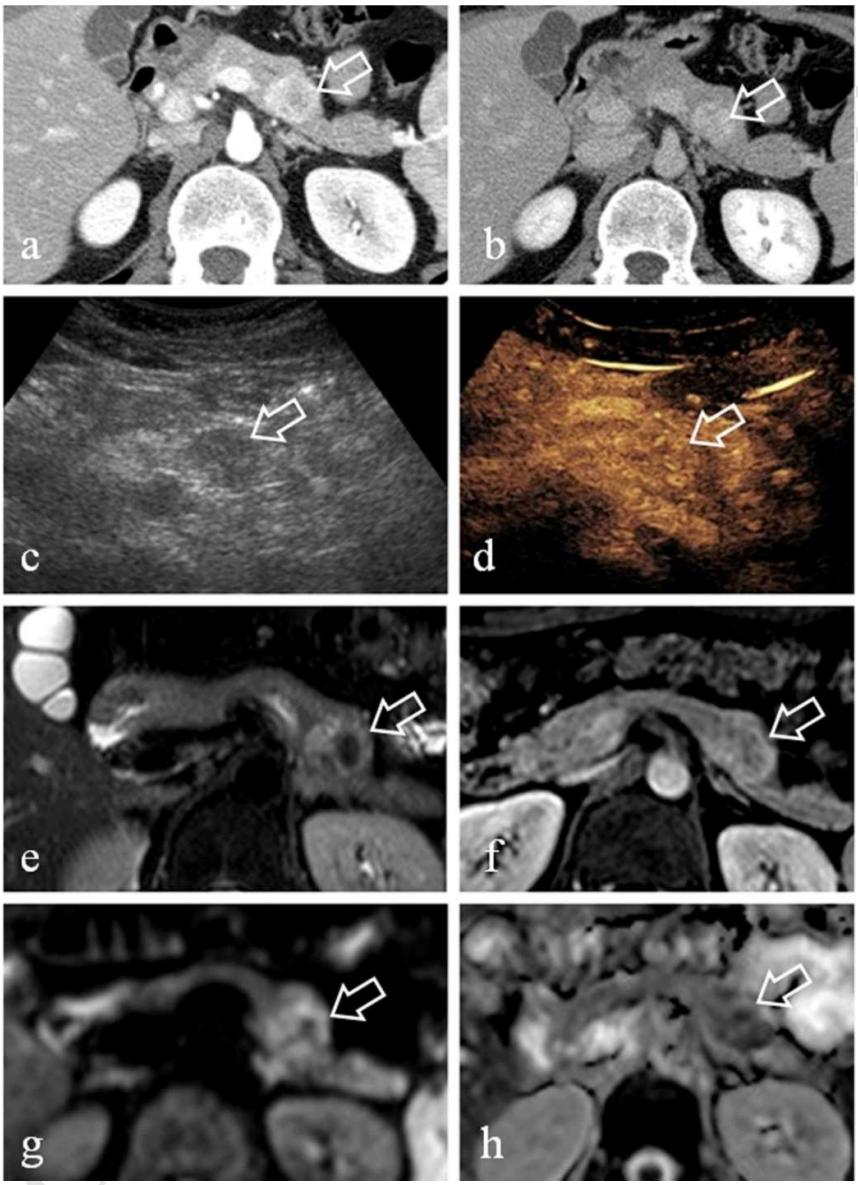

Figure 6. 34-years-old male patient with incidental finding of non-functioning pancreatic neuroendocrine tumor (arrow). Mixed phase at 64-slice Split-bolus CT protocol (a) shows a well defined lesion that exhibits intense enhancement which persists into the delayed phase (b) in the tail of the pancreas. US (c) shows a hypoechoic lesion and CEUS (d) demonstrates hyperenhancing pattern at the early phase. At 3 T MRI evaluation on T2W images the NET appears as slightly inhomogeneous hyperintense lesion (e) that exhibits intense enhancement at arterial phase T1W breath-hold fat-suppressed 3D gradient-echo images after intravenous administration of gadolinium (Gd-DTPA) (f). On DWI with b=1000 values (g) and ADC map (h) the tumor (arrow in g and h) *show* restriction *to water* diffusion due *to increased cellular* density.

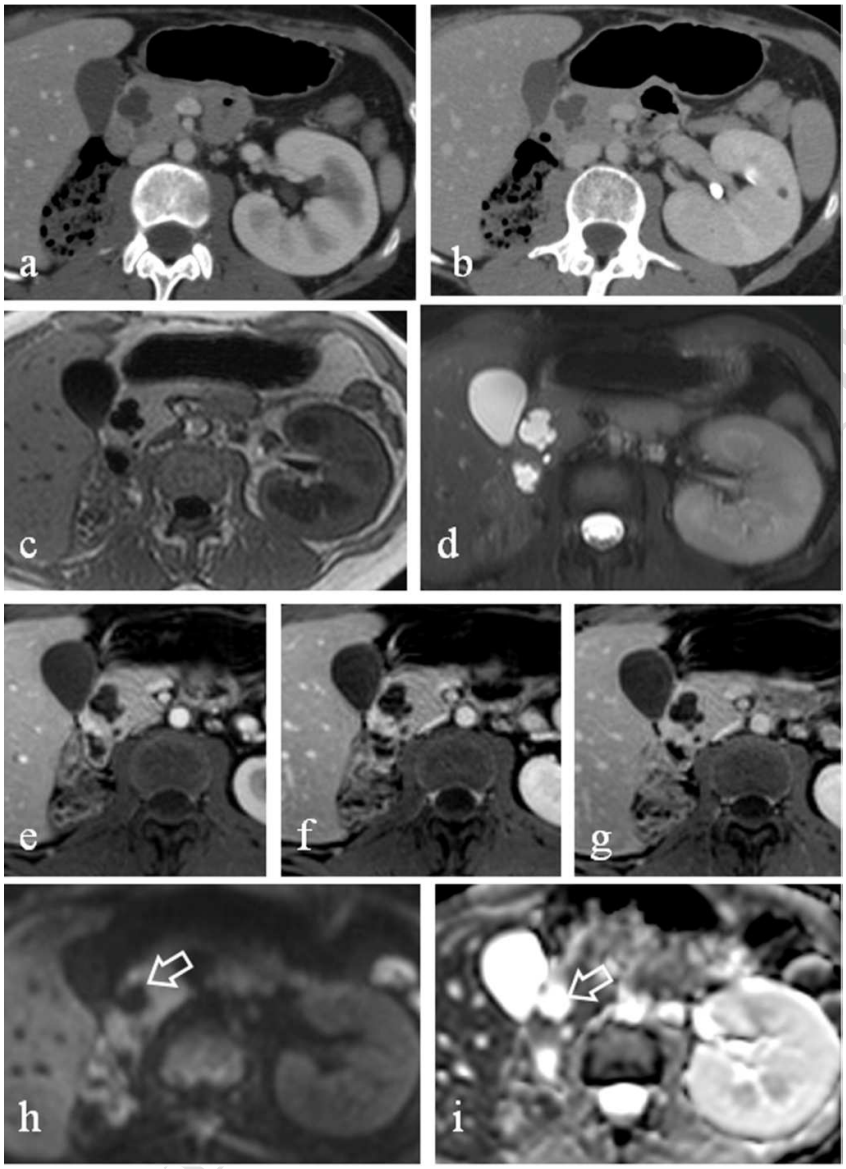

Figure 7. 29-years-old female patient with serous cystadenoma. Mixed phase at 64-slice Split-bolus CT protocol (a) and delayed phase (b) show a cystic lesion with polycyclic contours and some thin internal septa with no significant enhancement in the head of the pancreas. 3 T MRI on T1W (c) and fat suppressed T2W images (d) confirm the cystic formation. At multiphase T1W breath-hold fat-suppressed 3D gradient-echo images after intravenous administration of gadolinium (Gd-DTPA) (e-g) thin internal septa doesn't exhibit significant enhancement. On DWI with b=1000 values (h) and ADC map (i) the lesion not demonstrated restriction of the diffusion of the water molecules.

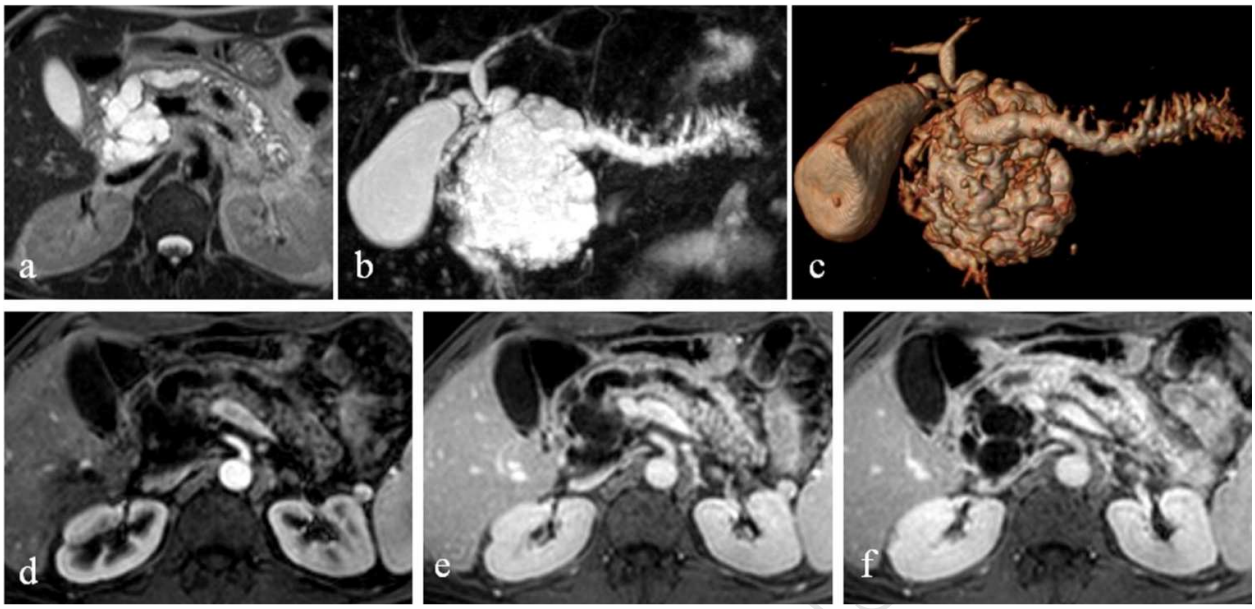

Figure 8. 37-years-old female patient with macrocystic serous cystadenoma at 1.5 T MRI. T2W images (a), MRCP (b), and MRCP sequences with 3D reconstruction (c) show a well-defined voluminous cystic lesion with internal septa and marked dilatation of the main pancreatic duct and the lateral ducts. The internal septa of the lesion exhibit progressive enhancement on multiphase T1W breath-hold fat-suppressed 3D gradient-echo images after intravenous administration of gadolinium (Gd-DTPA) (d-f).

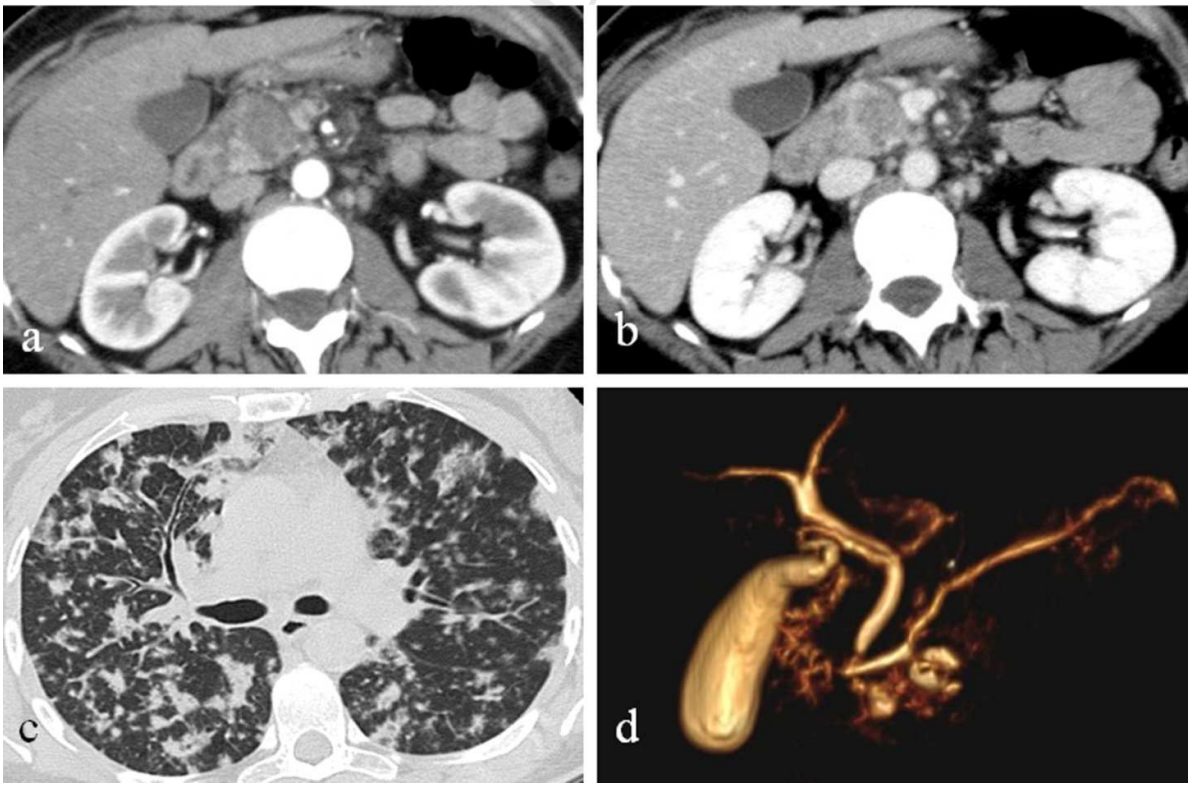

Figure 9. 56-years-old female patient with mucinous adenocarcinoma of the pancreas. Pancreatic parenchymal phase (a) and portal-venous phase (b) at MDCT show hypodense lesions in the head/uncinate process of the pancreas. CT of the chest show multiple diffuse bilateral parenchymal metastasis (c). No communication with pancreatic duct at 1.5 T MRCP imaging with 3D reconstruction was demonstrated (d).

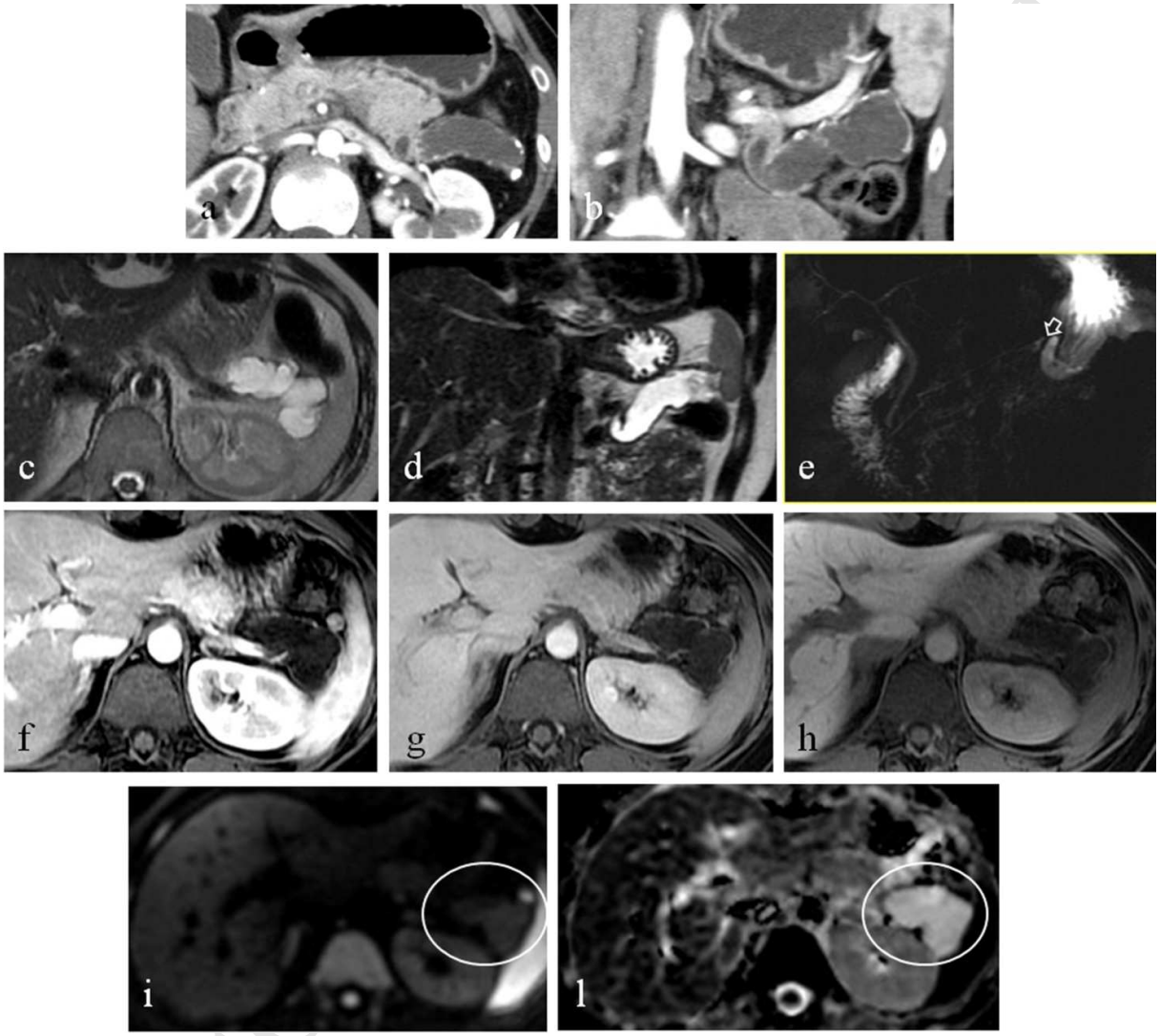

Figure 10. 36-years-old female patient with main-duct intraductal papillary mucinous neoplasm. Axial a) and coronal multiplanar reconstruction (b) mixed phase at 64-slice Split-bolus CT protocol shows a significant cystic dilatation of the main pancreatic duct with linear parietal calcifications without mural nodules and/or areas of pathological enhancement. On 1.5 MRI the lesion appears homogeneously hyperintense on the axail (c) and coronal (d) T2W images, and site of communication with the Wirsung is recognizable on the MRCP sequences (arrow in e). At multiphase T1W breath-hold fat-suppressed 3D gradient-echo images after intravenous administration of gadolinium (Gd-DTPA) (f-h) the lesion doesn't exhibit enhancement neither restriction of diffusion on DWI with high b values (i) and ADC sequences (l).

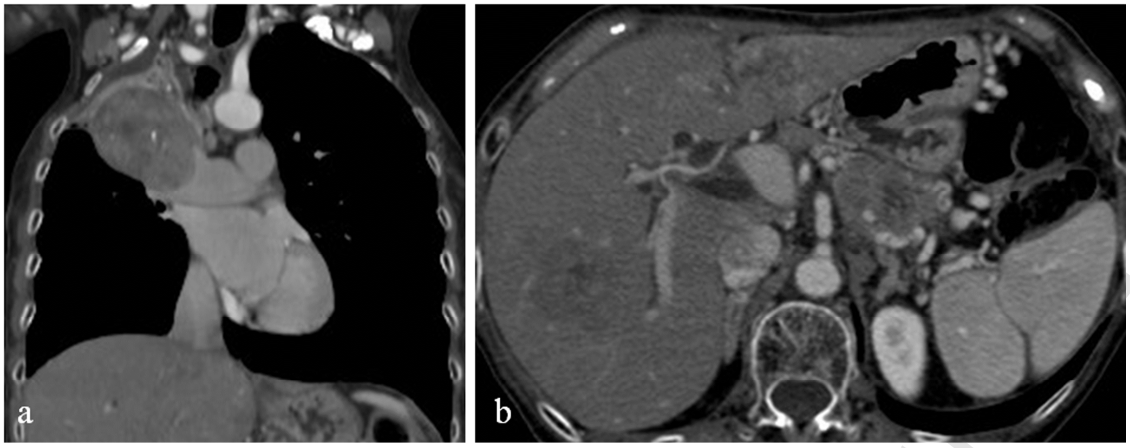

Figure 11: 75-years-old female patient with metastatic small cell lung cancer at 64-slice Split-bolus CT protocol during follow-up. Mixed phase shows the primitive inhomogeneous mass at the right upper lobe of the lung (a) and a heterogeneous metastasis in the liver and in the tail of the pancreas (b).

Figure 12. 56-years-old female patient with previous excision of malignant melanoma of the back. 64-slice CT during follow-up in axial arterial phase (a), venous phase (b) and coronal venous phase (c) shows a voluminous metastatic mass that exhibits inhomogeneous enhancement in the head of the pancreas with massive infiltration of adjacent vessels and structures.

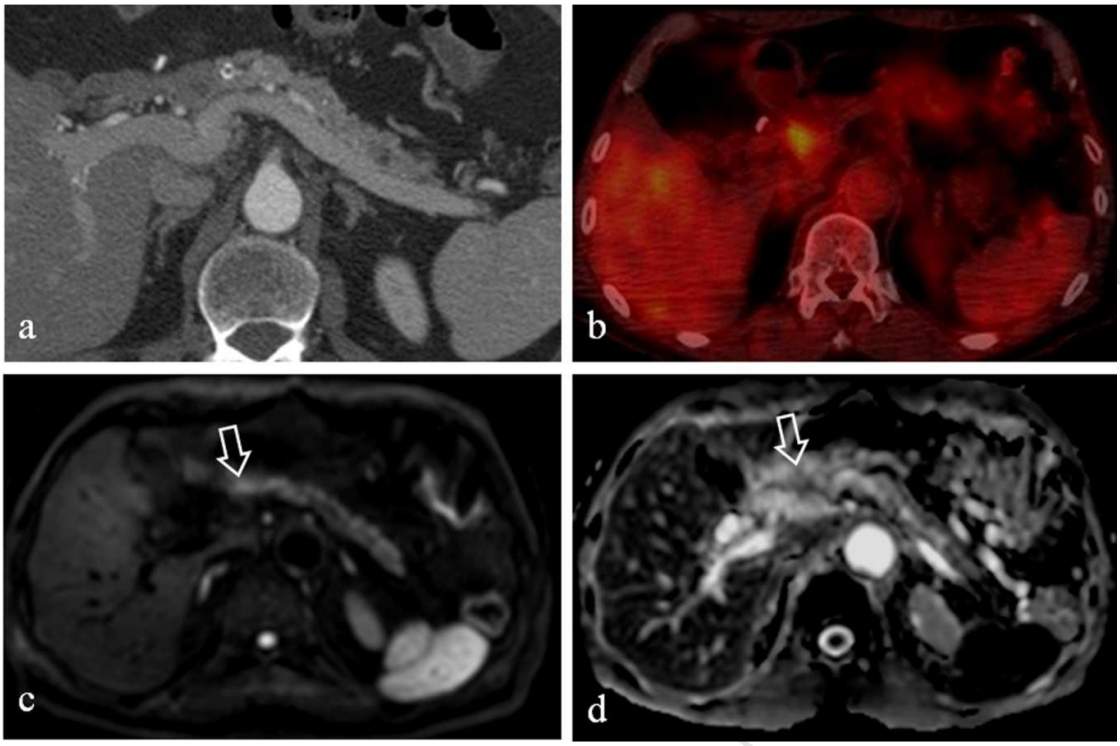

Figure 13. 79-years-old male patient with previous duodeno-cefalo pancreatectomy for neuroendocrine tumor of the head of the pancreas at 64-slice Split-bolus CT protocol post-surgery (a); after 12 months, 18F-FDG PET-TC (b) shows a small area of hyperfixation suspicious for recurrence, next to the surgical clip. 3 T mpMRI including DWI with b=1000 values (c) and ADC map (d), confirms the PET-TC finding showing a circumscribed area of restricition of diffusion (arrow in c and d).